This article was downloaded by: [Norges Landbrukshoegskole], [Dr Jorge Marchetti]
On: 20 April 2012, At: 03:35
Publisher: Taylor & Francis
Informa Ltd Registered in England and Wales Registered Number: 1072954 Registered office: Mortimer House, 37-41 Mortimer Street, London W1T 3JH, UK

Chemical Engineering Communications
Publication details, including instructions for authors and subscription information:
http://www.tandfonline.com/loi/gcec20

# REVIEW OF KERNELS FOR DROPLET-DROPLET INTERACTION, DROPLET-WALL COLLISION, ENTRAINMENT, RE-ENTRAINMENT, AND BREAKAGE

J. M. Marchetti [a] & H. F. Svendsen [a]

[a] Faculty of Natural Science and Technology, Chemical Engineering Department, Norwegian University of Science and Technology, Sem Sælands, Trondheim, Norway

Available online: 17 Feb 2012

To cite this article: J. M. Marchetti & H. F. Svendsen (2012): REVIEW OF KERNELS FOR DROPLET-DROPLET INTERACTION, DROPLET-WALL COLLISION, ENTRAINMENT, RE-ENTRAINMENT, AND BREAKAGE, Chemical Engineering Communications, 199:4, 551-575

To link to this article: http://dx.doi.org/10.1080/00986445.2011.592453

PLEASE SCROLL DOWN FOR ARTICLE

Full terms and conditions of use: http://www.tandfonline.com/page/terms-and-conditions

This article may be used for research, teaching, and private study purposes. Any substantial or systematic reproduction, redistribution, reselling, loan, sub-licensing, systematic supply, or distribution in any form to anyone is expressly forbidden.

The publisher does not give any warranty express or implied or make any representation that the contents will be complete or accurate or up to date. The accuracy of any instructions, formulae, and drug doses should be independently verified with primary sources. The publisher shall not be liable for any loss, actions, claims, proceedings, demand, or costs or damages whatsoever or howsoever caused arising directly or indirectly in connection with or arising out of the use of this material.

Chem. Eng. Comm., 199:551–575, 2012
Copyright © Taylor & Francis Group, LLC
ISSN: 0098-6445 print/1563-5201 online
DOI: 10.1080/00986445.2011.592453

Taylor & Francis
Taylor & Francis Group

Downloaded by [Norges Landbrukshoegskole], [Dr Jorge Marchetti] at 03:35 20 April 2012

# Review of Kernels for Droplet-Droplet Interaction, Droplet-Wall Collision, Entrainment, Re-entrainment, and Breakage

J. M. MARCHETTI AND H. F. SVENDSEN

Faculty of Natural Science and Technology, Chemical Engineering Department, Norwegian University of Science and Technology, Sem Sælands, Trondheim, Norway

*Gas purification is one of the most common and important process steps in combined oil and gas production in order to obtain a product meeting the required export specifications. One of the separation steps is droplet removal, which may be found in several positions in a gas processing train. Gas dehydration, sweetening, and, in particular, compression are very dependent on an almost droplet-free gas. The equipment normally used for this purpose is a so-called scrubber, where the droplets are usually removed in three stages. The process of droplet removal is governed by several physical phenomena, such as droplet-droplet interaction, droplet deposition on dry and wet walls, droplet re-entrainment by the gas flow, coalescence, and breakage. For each of them closure laws are needed, and several kernels have been developed in order to establish in what operational domain and under which specific conditions the various phenomena dominate, can be minimized, or can be eliminated this article is a review of the individual physical processes, and the models developed to describe these including advantages and shortcomings of each of them.*

**Keywords** Gas purification; Kernels; Scrubbers

## Introduction

Natural gas is one of the main fossil fuels in use today and has a large range of applications. It is employed as fuel for power production and as raw material in the petrochemical industry. At present it represents 30% of the fossil energy used worldwide (BP, 2006). Its composition is mainly methane, ethane, propane, and butane, with small amounts of nitrogen, carbon dioxide, pentane, and higher hydrocarbons (Kolev, 2002).

In the production of natural gas, which nearly always is produced together with oil or condensate, many steps of purification and processing are needed to meet export specifications. Separation of liquid droplets from the gas phase often takes place in many locations in a gas processing chain and is a prerequisite for stable operation of dehydration, acid gas removal, and recompression stages. It is a vital step, as a dispersed phase might produce foaming and poor operation in dehydration and sweetening plants, and, even worse, erosion and breakdown of rotating

Address correspondence to J. M. Marchetti, Faculty of Natural Science and Technology, Chemical Engineering Deptartment, Norwegian University of Science and Technology, Sem Sælands v. 4 NO-7491, Trondheim, Norway. E-mail: jorge.marchetti@chemeng.ntnu.no

equipment. Gas-liquid separation is normally carried out in verticals vessels called scrubbers that operate in a wide range of pressures (atmospheric to 200 bar) and temperatures (<200°C).

Several types of scrubbers are in use in the industry, depending on the operating conditions and the needed separation efficiency. Examples are:

- Electrostatic precipitators, which can have three main designs: (i) gas flowing up or down and droplets entering form the top, (ii) gas flowing horizontally while droplets enter perpendicularly to the gas, and (iii) droplets injected into a venturi nozzle
- Diffusion separators
- Impingement separators
- Packed bed separators
- Wave plate separators
- Cyclones
- Wire and fiber filters
- Swirl flow separators
- Wet scrubbers (Bürkholz, 1989)

The scrubber used for droplet removal normally has three main parts: an inlet vane, a mesh pad, and a cyclone section in order to produce the separation according to specifications. A sketch of a scrubber is found in Figure 1.

The main purpose of the inlet section/inlet vane is to reduce the momentum of the fluid and to produce a separation of large droplets from the gas. Together with the inlet valve, it also reduces the pressure of the inlet stream. It is normally mounted horizontally in the scrubber and is designed as a zigzag vane pack redirecting the gas and separating the droplets by impaction. As a second step, a mesh pad is normally used. This part of the equipment consists of layers or rolls of wires with the aim of separating

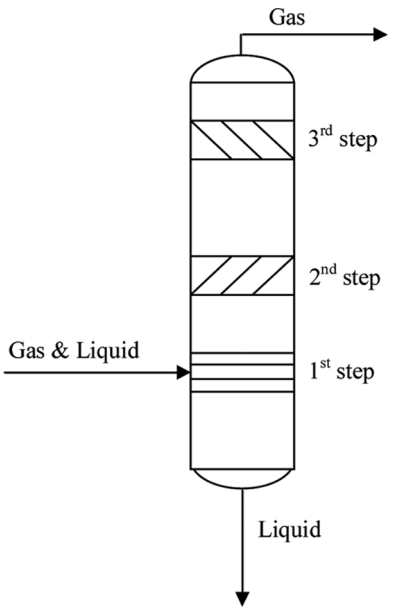


**Figure 1.** A typical scrubber and its three main sections.

Downloaded by [Norges Landbrukshoegskole], [Dr Jorge Marchetti] at 03:35 20 April 2012

Downloaded by [Norges Landbrukshoegskole], [Dr Jorge Marchetti] at 03:35 20 April 2012

medium-size droplets from the gas flow. Another of its functions, often encountered at high pressure, is to work as a coalescer, increasing droplet sizes. Finally, in the upper part of the scrubber there is a bank of cyclones where the g-forces separate the small droplets by interaction with the walls and enables liquid drainage down to the bottom of the scrubber. The exit gas stream should be dry and according to specifications. Often the separation cannot be done at high pressure, and a decompression stage is inserted, followed by separation and subsequent recompression before further transport by the gas pipelines (BP, 2006; Kolev, 2002; Austrheim et al., 2007, 2008a, 2008b; Johnsen, 2007; Dorao et al., 2008; Kidnay and Parrish, 2006).

In this equipment, several physical phenomena could take place simultaneously depending on operating conditions, physical properties, and separation specifications. Entrainment, droplet-wall interaction, and others are important physical phenomena that take place and that may create problems at higher pressure. Significant research has been performed over the past decades in order to understand the physics behind these phenomena and to enable predictions and quantification through so-called closure laws or kernels.

In this work, a review of the main research done and correlations obtained for entrainment, droplet-wall interaction, droplet breakage, and droplet-droplet collision frequency and their possible outcomes is presented and discussed. The focus it is to compare and discuss advantages and disadvantages of the kernels developed.

## Breakage

Breakage is defined as when a droplet splits into smaller daughter droplets. This could result in two new droplets (binary breakage) or in multiple droplets (more than two daughter droplets are produced). This phenomenon is relevant in gas purification as droplets break up both in the inlet vane and the mesh pad sections of a scrubber. It is vital to know the behavior of the droplets, the collision outcomes, and the resulting size distribution with the aim of being able to predict the overall performance of the equipment. Figure 2 shows the breakage for binary and ternary scenarios. For the ternary scenario, two different possibilities are presented.

Binary breakage is the most studied case due to its apparent simplicity and because it can be associated with parameters of the system and/or geometrical properties of the droplets. The breakage can occur through many droplet movement modes, such as vibrational, bag breakup, bag and stamen breakup, sheet stripping, wave crest stripping, and catastrophic breakup. Each of them has been explained elsewhere (Kolev, 2002). However, the main parameter used to determine what kind

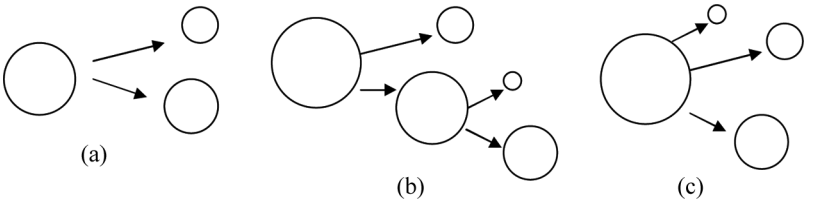


**Figure 2.** Different types of breakage: (a) binary breakage, (b) ternary breakage where a daughter of the first is father of the second breakage, and (c) ternary breakage where one father gives three daughters.

of breakup will take place is universally taken to be the Weber number:

$$We = \frac{\rho v^2 l}{\sigma} \tag{1}$$

Following Gelfand (1996), the transition from one fragmentation mode to another is presented in Table I.

The most studied breakage environment is breakage in turbulent flow. The research has focused on developing so-called breakup kernels or breakup rate expressions. Both expressions have similar meaning: a breakage rate is the rate at which breakage is produced, while a kernel is the mathematical expression that is associated with a distribution function; in our case, the breakage rate is a breakage kernel.

This use of these terms stem from the population balance equations, where, if considering a breakage dominated system, the steady-state population balance equation can be written as follows:

$$v_x \frac{\partial f(x,d)}{\partial x} = -b(x,d)f(x,d) + \int_d^{d_{\max}} h(d' \to d)b(x,d')f(x,d')dd' \tag{2}$$

where the left-hand side term represents the change in the population of a certain droplet size d due to loss (death) and production (birth). The death term is the first on the right-hand side, and the droplets are lost by breakage through a breakage rate b(x, d) multiplied by the fraction of all droplets having size $d$, f(x, d). The birth term is the second on the right-hand side and describes the change in the population of d through the creation of daughters of size $d$ from breakage of fathers of larger sizes. This last term has a distribution function that determines how droplets with size d′ are split into daughters; b(x, d′) is the breakage rate and h(d′(d) is the redistribution function.

Table II shows a summary of several models for breakage rates, either from physical properties or from inverse problem solutions (Patruno et al., 2009a, 2009b; Lasheras et al., 2002; Sathyagal et al., 1996; Ramkrishna, 2000). A more detailed description of these functions was made by Patruno et al. (2009b) and Lasheras et al. (2002). The functions predict the rate at which the droplets break into smaller droplets. However, they do not directly predict the size distribution of the daughter droplets. Several models for daughter size distributions have been developed. These are needed in order to have a complete expression for the breakup model, as shown in several studies, e.g., Patruno et al. (2009b).

As can be seen from Table II, each model has different assumptions and restrictions, based on the setup and case studied. These differences make it almost impossible to have an objective comparison between models since to compare them a experimental setup should be chosen, and this will benefit some models over others, not

**Table I.** Breakup mode according to Weber number range

| Fragmentation mode | Weber number range |
|---|---|
| Vibration | <12 |
| Bag | 12–50 |
| Bag and stamen | 50–100 |
| Sheet stripping | 100–350 |
| Wave crest and catastrophic breakup | >350 |

Downloaded by [Norges Landbrukshoegskole], [Dr Jorge Marchetti] at 03:35 20 April 2012

Downloaded by [Norges Landbrukshoegskole], [Dr Jorge Marchetti] at 03:35 20 April 2012



**Table II.** Summary of some breakage rate functions b(d), number/time

| Mathematical Expression | Assumptions-limitations | Reference |
|---|---|---|
| $b(d) = \frac{k_1}{d^{2/3}} \exp\left(-\frac{k_2}{d^{5/3}}\right)$ | The authors assumed that the surface energy was $\bar{E} = c_2 \rho \varepsilon^{2/3} d^{11/3}$ and the breakage time was given by $t_b \propto d^{2/3} \varepsilon^{-1/3}$ | Coulaloglou and Tavlarides (1977) |
| $b(d) = C_k \frac{\sqrt{\Delta u^2(d)}}{d} \int_{u*}^{\infty} 3\sqrt{\frac{6}{\pi}} x^2 \exp\left(-\frac{3x^2}{2}\right) dx$ | The probability was based on a Maxwell distribution function | Konno et al. (1980) |
| $b(d) = k_g \frac{\sqrt{\beta(\varepsilon d)^{2/3} - 12\sigma/(\rho d)}}{d}$ | Viscous forces and turbulent stress overcoming deformation energy were neglected | Martínez-Basán et al. (1999) |
| $b(d) = \int_0^{10\pi/d} \frac{0.14\pi}{16} \left(d + \left(\frac{2\pi}{k}\right)^2\right) \left(d^{2/3} + \left(\frac{2\pi}{k}\right)^{2/3}\right)^{1/2} \varepsilon^{1/3} \times \exp\left(-\frac{1.18}{(2\pi)^{2/3}} \frac{\sigma k^{2/3}}{\rho d \varepsilon^{2/3}}\right) k^2 dk$ | Similar to Konno et al. (1980), but the breakup is produced as a result of collision between particles and turbulent eddies | Prince and Blanch (1990) |
| | Similar to Prince and Blanch (1990) with a difference in the calculation of the activation energy $E_c$ | Tsouris and Tavlarides (1994) |

(*Continued*)

Downloaded by [Norges Landbrukshoegskole], [Dr Jorge Marchetti] at 03:35 20 April 2012

**Table II.** Continued

| Mathematical Expression | Assumptions-limitations | Reference |
|---|---|---|
| $b(d) = C_{t1}\int_{n_e} \pi\left(\frac{2}{k}+d\right)^2 \left(8.2\varepsilon^{2/3}k^{-2/3}+1.07\varepsilon^{2/3}d^{2/3}\right)^{1/2} \times \exp\left(\frac{C_{t2}E_c}{0.43\rho\pi\varepsilon^{2/3}\left(\frac{2}{k}\right)^{11/3}}\right) dn_e$ | | |
| $\frac{\Omega_B(\upsilon:\upsilon f_{BV})}{(1-\varepsilon_d)n} = C\left(\frac{\varepsilon}{d^2}\right)^{1/3}\int_{\xi_{\min}}^{1}\frac{(1+\xi)^2}{\xi^{11/3}} \times \exp\left(-\frac{12\sigma c_f}{\beta\rho_c\varepsilon^{2/3}d^{5/3}\xi^{11/3}}\right)d\xi$ | Have no unknown parameters since the constants are determined from turbulence theory | Luo and Svendsen (1996) |
| *total breakage rate* | | |
| $\Omega_B(\upsilon) = \frac{1}{2}\int_0^1 \Omega_B(\upsilon:\upsilon f_{BV})\ df_{BV}$ | | |
| $b(d) = \frac{Amp}{\sqrt{2\pi}\omega d}\exp\left(-\frac{\ln(d/d_c)^2}{2\omega^2}\right)$ | Inverse problem solution; therefore, problem dependent | Patruno et al. (2009b) |
| $b(d) = \sqrt{\frac{\sigma}{\rho v}}\left\{0.422\exp\left\{-0.24775\ln\left(We\left(\frac{\pi d^3}{6D^3}\right)^{5/9}\left(\frac{\mu_c}{\mu_d}\right)^{0.2}\right)^2 + 2.15475\ln\left(We\left(\frac{\pi d^3}{6D^3}\right)^{5/9}\left(\frac{\mu_c}{\mu_d}\right)\right)\right\}\right\}$ | Inverse problem solution; therefore, problem dependent | Sathyagal et al. (1996) |

allowing a critical comparison of them. Furthermore, inverse model problems are impossible to compare.

According to Lasheras et al. (2002) three approaches were historically formulated for the prediction of the daughter size distribution term, $h(d, d_0)$: statistical models, phenomenological models, and hybrid models.

Valentas et al. (1996) proposed two model scenarios. In the first case a father droplet gives two daughters of the same size, i.e., a very deterministic result. The second scenario considered that a father droplet could give a distribution of possible daughter sizes. In this case the probability for a father droplet of size $d_0$ to form a daughter droplet of size d, was predicted to have the following expression:

$$h(d, d_0) = \frac{1}{\tau\sqrt{2\pi}} \exp\left(-\frac{(d-\overline{d})^2}{2\tau^2}\right) \tag{3}$$

where $\overline{d} = \frac{(d_0)^{2/3}}{m}$, and $m$ is the number of daughters produced. In this case the functionality follows a normal distribution.

Coulaloglou and Tavlarides (1977) used the previous model and fixed the values of m and $\sigma$. In their case the final expression was:

$$h(d^3, d_0^3) = \frac{2.4}{d_0^3} \exp\left(-\frac{-4.5(2d^3 - d_0^3)^2}{d_0^6}\right) \tag{4}$$

Hsia and Tavlarides (1983) used a beta distribution (see Figure 3) instead of a Gaussian distribution or a truncated normal distribution in their daughter size distribution function. Their expression is as follows:

$$h(d^3, d_0^3) = \frac{30}{d_0^3}\left(\frac{d^3}{d_0^3}\right)^2\left(1 - \frac{d^3}{d_0^3}\right)^2 \tag{5}$$

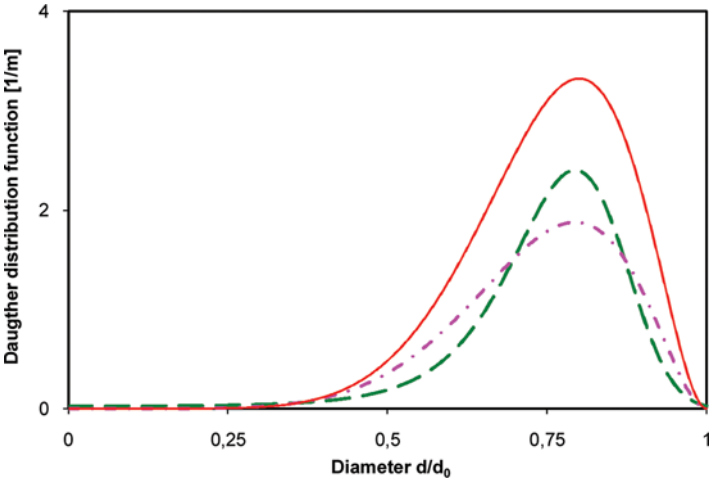


**Figure 3.** Comparison of h functions: (– – –) Coulaloglou and Tavlarides (1977), (–·–) Hsia and Tavlarides (1983), (—) Konno et al. (1983). (Figure provided in color online.)

Downloaded by [Norges Landbrukshoegskole], [Dr Jorge Marchetti] at 03:35 20 April 2012

A more general expression using a beta distribution approximation was developed by Lee et al. (1987). In their expression two new parameters, $a$ and $b$, were added and calculated from experimental information.

$$h(d^3, d_0^3) = \frac{\Gamma(a+b)}{\Gamma(a)\Gamma(b)d_0^3}\left(\frac{d^3}{d_0^3}\right)^{a-1}\left(1-\frac{d^3}{d_0^3}\right)^{b-1} \tag{6}$$

Konno et al. (1983) proposed a hybrid model with a statistical model as the basis, but the energy distribution among turbulent eddies was also included. Also, only binary breakup was assumed and that each father will produce equal-size daughters. The final expression was:

$$h(d, d_0) = \frac{\Gamma(12)}{\Gamma(3)\Gamma(9)d_0}\left(\frac{d}{d_0}\right)^8\left(1-\frac{d}{d_0}\right)^2 \tag{7}$$

Hesketh et al. (1991) proposed a model using a 1/X-type distribution in order to have a prediction that will give a daughter size distribution between that predicted by random breakage and that by coalescence-breakage. This model has two constants, one needed for normalization (I) and the other obtained empirically (B). The final equation is as follows:

$$h(d^3, d_0^3) = \left(\frac{1}{\left(B+(d/d_0)^3\right)}+\frac{1}{\left(1+B-(d/d_0)^3\right)}-\frac{2}{(B+0.5)}\right)\frac{I}{d_0^3} \tag{8}$$

Martínez-Basán et al. (1999) proposed that the creation of daughter droplets of a certain diameter is proportional to the turbulent stresses associated with the length scale of each droplet size. This gives:

$$h(d, d_0) = \frac{1}{d_0}\frac{\left(\frac{1}{2}\rho\beta(\varepsilon d_0)^{2/3}\right)^2\left(\alpha^{2/3}-\delta^{5/3}\right)\left(\left(1-\alpha^3\right)^{2/9}-\delta^{5/3}\right)}{\int_{\alpha_{\max}}^{\alpha_{\min}}\left(\frac{1}{2}\rho\beta(\varepsilon d_0)^{2/3}\right)^2\left(\alpha^{2/3}-\delta^{5/3}\right)\left(\left(1-\alpha^3\right)^{2/9}-\delta^{5/3}\right)d\alpha} \tag{9}$$

where $\alpha = \frac{d}{d_0}$ and $\delta = \frac{d_c}{d_0}$.

Other approaches to obtain droplets size distributions are based on phenomenological approaches. Several distribution functions have been obtained, such as the ones developed by Nambiar et al. (1992), Tsouris and Tavlarides (1994), Luo and Svendsen (1996), and Martínez-Basán et al. (1999), among others. The Luo and Svendsen (1996) model, as well as that of Tsouris and Tavlarides (1994), are based on energy arguments. The Luo and Svendsen model (1996) provides an overall breakage rate and a "partial" breakage rate. The mathematical expression, normalized, is:

$$h(vf_v, v) = \frac{2\int_{\xi_{\min}}^1 (1+\xi)^2\xi^{-11/3}\mathrm{e}^{-\chi_c}d\xi}{v\int_0^1\int_{\xi_{\min}}^1 (1+\xi)^2\xi^{-11/3}\mathrm{e}^{-\chi_c}d\xi df_v} \tag{10}$$

where $v = \frac{\pi d_0^3}{6}$ is the volume of the father droplet and $vf_v = \frac{\pi d_1^3}{6}$ is the volume of the daughter, $\xi = \frac{d_0}{d}$ is the eddy/droplet diameter ratio, and $\chi_c = \frac{12C_f\sigma}{\beta\rho\varepsilon^{2/3}d^{5/3}\xi^{11/3}}$ is the critical energy required for breakage.

Downloaded by [Norges Landbrukshoegskole], [Dr Jorge Marchetti] at 03:35 20 April 2012

Kernels based on inverse modeling have also been obtained, as by Sathyagal et al. (1996) and Patruno et al. (2009b). In these procedures, the solution will be problem dependent and not easily generalized. However, the solutions of many inverse problems could be correlated with empirical equations. Sathyagal et al. (1996) found the following expression:

$$h(d, d_0) = \frac{b\frac{d_0^3}{d^3}}{\left(1 - \frac{\Phi}{4}\right) + \frac{\Phi}{4\left(d_0^3/d^3\right)^4}} \tag{11}$$

where $\ln \Phi = 0.0577 \ln\left(\frac{\mu_c}{\mu_d}\right) - 0.558$.

In conclusion, it can be seen that there are different approaches to obtaining a breakage kernel, based on the nature of problem itself or on its properties or as a solution to the inverse problem. Inverse solutions are problem dependent, and a large number of them must be obtained to be able to correlate them and get general expressions. However, the time required to perform these calculations it is very short, and therefore they are not time consuming.

All the previous kernels for droplet breakup size distribution can be divided in two main categories, related to the outcome of the breakage. This result is related to the mass and volume fractions of each daughter. In the models of Coulaloglou and Tavlarides (1977), Hsia and Tavlarides (1983), and Konno et al. (1983), the daughter droplet size distributions are shown in Figure 3. As can be seen, the most frequent, or likely, ratio between daughter and father diameters is 0.79, indicating that there is a high probability of having breakage in two equal mass droplets.

The second main group predicts high probabilities for droplets with one size close to the father droplet and one very small daughter. This distribution is predicted by the models of Luo and Svendsen (1996) and by Hesketh et al. (1991). In the latter case, presented in Figure 4, it can be seen that the possibility of having two equal mass droplets is zero, and the high probabilities are towards the extremes of the x-axis.

All these models have several limitations with regard to their applicability to a more general problem of breakage, when no a priori assumption is made on the number of daughters produced and where higher order breakage could be possible.

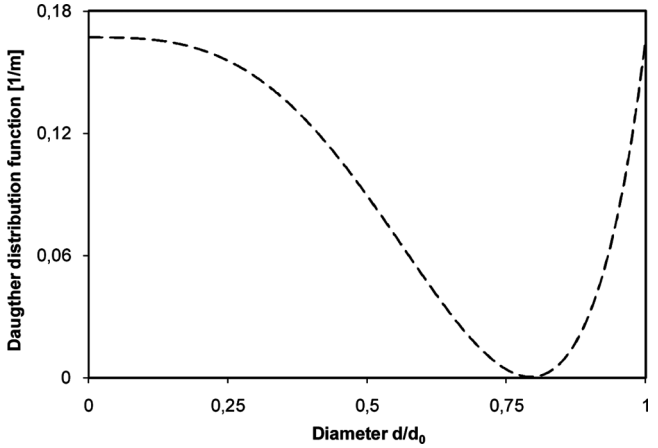


**Figure 4.** Variations of the h function: (– – –) Hesketh et al. (1991).

Downloaded by [Norges Landbrukshoegskole], [Dr Jorge Marchetti] at 03:35 20 April 2012

This problem has not been completely resolved yet due to its complexity. In addition, there is a problem that many of these kernels, when used to verify both the mass balance and the particle number balance, do not satisfy both criteria perfectly. The expressions by Coulaloglou and Tavlarides (1977) and Hesketh et al. (1991) do satisfy both balances but not the rest, producing an average number of daughter droplets slightly larger than two, even when considering only binary breakage.

As pointed out before, each expression shown above is experimentally case dependent, not giving us an easy task when making a comparison among them.

Downloaded by [Norges Landbrukshoegskole], [Dr Jorge Marchetti] at 03:35 20 April 2012

## Collisions Between Droplets

In gas purification systems, droplets are normally in very low volume fractions in the gas medium. However, in turbulent flows the collision frequency can be reasonably high. In addition, since surfaces with liquid films are the normal capture medium, these processes are important. The collision rate and its description are well established in Jakobsen (2008). In this section the focus will be on the outcomes of the droplet/droplet interactions.

A collision between two equal-sized droplets is the phenomenon most studied, and it has been found that several outcomes are possible depending on the collision Weber number and the so-called impact factor; see Figure 5. The impact factor is defined as $Ip = L/d$, the ratio of the distance between the droplet centers perpendicular to the flow direction of the droplets and the droplet diameter (Jakobsen, 2008; Orme, 1997; Kollár et al., 2005; Gotaas et al., 2007a).

Figure 6 shows an example of possible outcomes of the interaction between two droplets as a function of the Weber number and the impact factor (B). The main regimes observed are bouncing and coalescence.

An extensive description of each regime was obtained by Qian and Law (1997). The authors did an intensive study of binary droplet collisions focusing on the five possible collision outcomes at several operational pressures. The five possible outcomes are: (I) coalescence after a small deformation produced by the collision, (II) bouncing where both droplets maintain their shape and size after the interaction, (III) coalescence after a major deformation of both droplets, (IV) the droplets coalesce but afterwards separate because of very high impact momentum, and (V) the droplets coalesce and separate by stretching separation.

### *Coalescence (Regions I and III)*

This phenomenon takes place when two droplets approach each other with an energy that will not produce bouncing, but a weak interaction, which after a small separation will end in forming a cylinder that will finally take the shape of a droplet.

A schematic of this behavior can be seen in Figure 7.

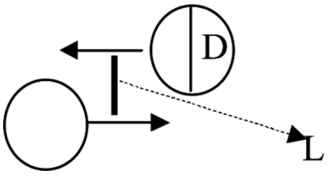


**Figure 5.** Impact factor between two droplets.

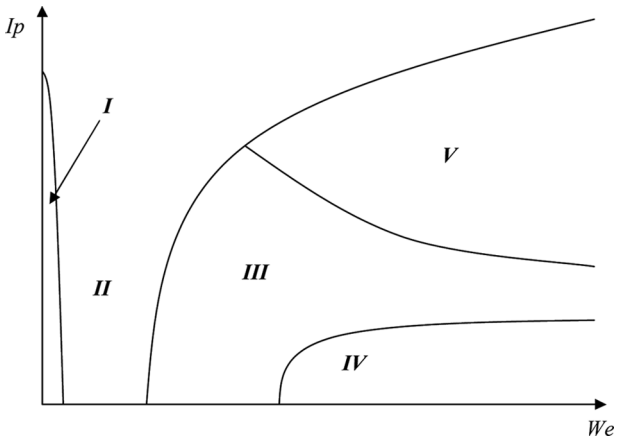


**Figure 6.** Schematic representation of possible outcomes from binary collisions. The regimes are: (I) coalescence, (II) bouncing, (III) coalescence, (IV) near head-on separation, and (V) off-center separation (Gotaas et al., 2007a; Qian and Law, 1997).

Figure 7 can be described in five steps. Step A corresponds to the approach of the droplets to each other. At B both droplets interact with each other during the collision. C is the coalescence itself. In step D both droplets try to bounce from each other but do not have enough energy to separate, therefore step E takes place, where a new droplet is produced from the two previous ones. The spherical geometry is then established due to its lower Gibbs free energy.

Several studies have been done in order to understand the coalescence of two droplets. Qian and Law (1997) studied the interaction and outcomes of water and hydrocarbon droplets in several gas environments. The authors found that the hydrocarbon droplet has a greater tendency to coalesce when the gas phase has some amount of hydrocarbon in it.

Coulaloglou and Tavlarides (1977) proposed coalescence efficiencies and collision frequencies based on the size and volumes of the droplets. Multiplication of these two values will give the coalescence rate. Both expressions are:

Collision frequency

$$h(d_1, d_2) = C\frac{\varepsilon^{1/3}}{1+\phi}(d_1 + d_2)^2\left(d_1^{2/3} + d_2^{2/3}\right)^{1/2} \tag{12}$$

Coalescence efficiency

$$\lambda(d_1, d_2) = \exp\left(C\frac{\varepsilon\rho_c\mu_c}{\sigma^2(1+\phi)^3}\left(\frac{d_1 d_2}{d_1 + d_2}\right)^4\right) \tag{13}$$

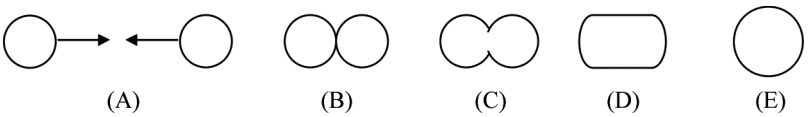


**Figure 7.** Time process of droplet coalescence.

Downloaded by [Norges Landbrukshoegskole], [Dr Jorge Marchetti] at 03:35 20 April 2012

Downloaded by [Norges Landbrukshoegskole], [Dr Jorge Marchetti] at 03:35 20 April 2012

Here $k$, $p$ are constants and $\rho_c$, $\mu_c$, $\sigma$ are the density, viscosity, and interfacial tension between the phases respectively.

However, according to Sovova (1981), the previous equations will over-predict small droplet coalescence compared to large droplet interactions. Therefore, Sovova (1981) proposed an energy-based coalescence efficiency. The author obtained the following expression, which predicts not only the coalescence of small droplets, but also the coalescence of larger droplets:

$$\lambda\left(d^3, d_0^3\right) = \exp\left(-C\frac{\sigma\left(d^2 + d_0^2\right)}{\rho_d N^2 D_i^{4/3}\left(d^{11} + d_0^{11}\right)}\right) \tag{14}$$

Similar to the Coulaloglou and Tavlarides (1977) model, Tsouris and Tavlarides (1994) proposed a new coalescence efficiency model based on the relation between the coalescence time and the contact time, in analogy to Chesters (1991). For two droplets to coalesce, the coalescence time, which is the time the film needs to drain and for rupture to take place, should be shorter than the contact time. Defining coalescence time T and contact time t, the authors obtained the following final expression:

$$\lambda(d_1, d_2) = \exp\left(\frac{6\pi\mu_c c_2 \zeta}{\rho_c \varepsilon^{*2/3}(d_1 + d_2)^{2/3}}\frac{31.25ND_i}{(T^2H)^{1/3}}\right) \tag{15}$$

Here the $C_2$ value is 3.44 to best fit the experimental information.

This model has, as well as the one proposed by Sovova (1981), one fitting parameter. This fitting parameter is obtained based on experimental data. Because of this, none of the models can be said to be general, but need to be fitted to the chemical system at hand. Even though a ternary interaction is very unlikely due to its low probability, none of these kernels could predict if it would happen.

### *Bouncing (II) and Outcomes (IV and V)*

This situation is achieved when the energy of each droplet is high enough to collide and rebound without producing coalescence. This phenomenon was seen experimentally by Gotaas et al. (2007a) and Qian and Law (1997), and when this would take place was predicted by Estrade et al. (1999) as a function of the Weber number:

$$We \geq \frac{8(3-\phi')}{\left(\cos\left(\sin^{-1}(\mathrm{B})\right)\right)^2\phi} \tag{16}$$

where

$$\phi = \left\{\begin{array}{ll} 1 - \frac{1}{4}(2-\pi)^2(1+\tau) & \text{for } Ip > 1/2 \\ \frac{\tau^2}{4}(3-\tau) & \text{for } Ip \leq 1/2 \end{array}\right\}$$

where $\tau = (1+\Delta)(1-I)$, $\phi' = 2\left(1+\frac{3}{\beta^2}\right)^{-2/3} + \left(1+\frac{3}{\beta^2}\right)^{1/3}$, $B = \left(\frac{d_1+d_2}{2}\right)(1-I)$, $I = sin(\Psi)$, and $\Psi$ is the angle between both centers and $\Delta = \mathrm{d}_1/\mathrm{d}_2$.

The parameter $\beta$ is considered as the critical ratio between the two radiuses above which the droplets are deformed because of the collision ($\beta = (d_1/d_2)_c$). It

Downloaded by [Norges Landbrukshoegskole], [Dr Jorge Marchetti] at 03:35 20 April 2012

was found that bouncing occurs when $\beta \leq$ ratio and that this ratio is attached to the material properties of both phases involved in the process.

According to Post and Abraham (2002) this model has two major drawbacks, one associated with the $\phi$ parameter. Its determination is experimental and therefore needs to be obtained for each experimental setup. The other is the simplification assumed regarding the interaction between the droplets and the fluids being disregarded.

Park et al. (2008) studied bouncing of droplets on a wall. They found that when the surface tension was reduced, and the Weber number thereby increased, the droplets did not retain their spherical form throughout the collision. Renardy et al. (2003) observed that when the droplets interacted with walls, waves appeared when $We\ Ca < 1$, where $Ca = v\ \mu/\sigma$.

In addition to bouncing itself, several outcomes are achievable in this process: head-on collision and rebound, head-on collision and partial rebound with satellite droplets, and collision with stretching separation; see Gotaas et al. (2007a, 2007b).

According to Pan and Suga (2005), reflexive separation occurs when the We number is extremely high and the value of $B = 0$ in the model described by Estrade et al. (1999), while the stretching separation occurs at high We numbers but with a value of $0.2 < B < 1$. These satellite droplet phenomena were found to be very diverse; several collisions might give singular satellite droplets and in other cases several smaller droplets were produced. Estrade et al. (1999) found that only one satellite droplet was formed in head-on collisions for $28 < We < 120$, while Ashgriz and Poo (1990) observed that as the Weber number increased, the amount of satellite droplets increased as well. The criterion used by Ashgriz and Poo (1990) for reflexive separation is as follows:

$$We > 3\left(7\left(1+\alpha^3\right)^{2/3} - 4\left(1+\alpha^2\right)\right)\frac{\alpha\left(1+\alpha^3\right)^2}{\alpha^6\eta_1 + \eta_2} \tag{17}$$

where $\eta_1$ and $\eta_2$ are fractions of the kinetic energy of the droplets, and

$$\eta_1 = 2\left(1-\xi^2\right)\left(1-\xi^2\right)^{1/2} - 1, \quad \eta_2 = 2\left(\alpha^2-\xi^2\right)^{1/2}(\alpha-\xi)^2 - \alpha^3 \text{ and } \xi = (1/2)Ip(1+\alpha)$$

where $\alpha$ is the collision angle.

This criterion is the most widely used and was employed by O'Rourke (1981), Tennison et al. (1998), Georjon and Reitz (1999), Estrade et al. (1999), Post and Abraham (2002), and Kollár et al. (2005). For stretching separation, these authors used the model developed by Brazier-Smith et al. (1972). This method assumes that there is no energy transferred to the gas from the droplets and the criterion is:

$$\frac{\nu^2 l\rho}{\sigma} = 3\Omega^{-2/3}\left(2 + \frac{\Omega}{\overset{+}{\varepsilon}}\ln\left(\frac{1+\overset{+}{\varepsilon}}{1-\overset{+}{\varepsilon}}\right) - 4\Omega^{2/3}\right) \tag{18}$$

where $\Omega$ is the axial diameter ratio and $\varepsilon^+$ eccentricity.

For stretching separation there are a few assumptions involved. When both droplets interact, a liquid ligament is produced and keeps the droplets together. When the separation is imminent, the radius of the liquid ligament becomes less than the radius of each droplet. No rotation is considered at any time. The ligament has

almost constant volume during the process. The number of satellite droplets that will be produced depends on the energy of the system and how far the droplets separate before the ligament breaks up. All the satellite droplets have the same kinetic velocity and the same mass.

Ashgriz and Poo (1990) developed a criterion for the boundary layer for stretching separation. They found the following expression:

$$We = \frac{4\left(1+\Delta^3\right)^2\left(3(1+\Delta)(1-x)\left(\Delta^3\Theta_2+\Theta_1\right)\right)^{1/2}}{\Delta^2\left(\left(1+\Delta^3\right)-(1-x^2)\left(\Delta^3\Theta_1+\Theta_2\right)\right)} \tag{19}$$

where

$$\tau \equiv (1-x)(1+\Delta)$$

$$\Delta = \frac{d_2}{d_1}$$

$$x = \frac{2Ip}{d_1+d_2}$$

$$\Theta_2 \begin{cases} 1-\frac{1}{4\Delta^3}(2\Delta-\tau)^2(\Delta+\tau) & \text{for } h > \frac{1}{2}d_2 \\ \frac{\tau^2}{4\Delta^3}(3\Delta-\tau) & \text{for } h < \frac{1}{2}d_2 \end{cases}$$

$$\Theta_1 \begin{cases} 1-\frac{1}{4}(2-\tau)^2(1+\tau) & \text{for } h > \frac{1}{2}d_1 \\ \frac{\tau^2}{4}(3-\tau) & \text{for } h < \frac{1}{2}d_1 \end{cases}$$

## Entrainment

Entrained droplets are produced by interaction between a gas stream and a fluid film. This process is important for mass and heat analysis in two-phase systems. Entrainment is typically produced due to the relative velocity of the gas phase and the film phase, meaning that it is not based on the velocity of the film or the velocity of the gas, but on the relative velocity of both phases. In this case, the gas will generate waves over the liquid to the point of producing droplets from it. These droplets are considered entrained. Figure 8 shows a schematic representation of a gas-driven case. However, it is important to note that entrainment could also occur under other physical geometries.

Several different models have been proposed but, considering its complexity, no general entrainment rate correlation that successfully reproduces all experimental information has been developed (Kataoka et al., 2000; Alipchenkov et al., 2004; Pan and Hanratty, 2002). Nevertheless, some correlations for entrainment rates have been reported and are summarized in Table III. Is it important to point out that other possible correlations are also available in the literature such as those from Lopez de Bertodano et al. (1997), Nigmatulin et al. (1996), Sawant et al. (2008), and Xie et al. (2004), among others.

For all the possible correlations predicting entrainment it is important to note that there is a limit to gas and liquid velocity below which entrainment will not take place at all. Normally this criterion is based on the relative velocity between the two

Downloaded by [Norges Landbrukshoegskole], [Dr Jorge Marchetti] at 03:35 20 April 2012

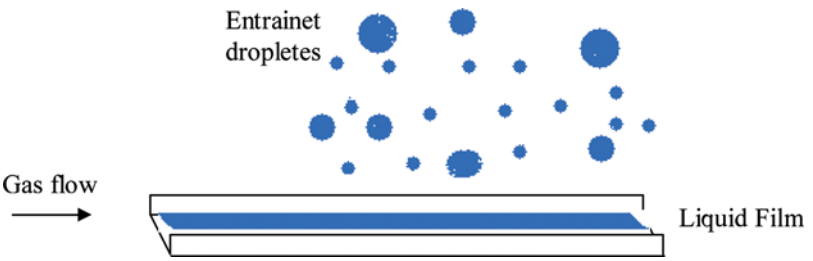


**Figure 8.** Schematic representation of an entrainment case. (Figure provided in color online.)

Downloaded by [Norges Landbrukshoegskole], [Dr Jorge Marchetti] at 03:35 20 April 2012

phases. Also, the correlations are experimentally determined, and therefore parameters may have to be recalculated in order to satisfy systems different from those for which the correlation was deduced.

Katoaka et al. (2000) proposed two different correlations based on different phenomena. Both expressions were obtained for steady state and are based on shearing off of roll wave crests by the gas core flow, making the entrainment dependent on the drag force. Although their expression is suitable for the entrance region with some error, a more detailed expression should be developed.

Different from the previous work, Ishii and Mishima (1989) developed their model for the fully developed region based on the Reynolds and Weber numbers. This model should, according to the authors, also satisfactorily correlate experimental information for the entrance, using a relaxation term to study in this region. However, the authors give a minimum value of the gas-phase Reynolds number below which this correlation should not be used. This value is 2 for vertical down-flows and 160 for horizontal or vertical up-flow systems. The only assumption made in this model is that the shearing off of roll wave crests is the dominant mechanism for liquid entrainment. No comment on the other mechanisms is presented.

Assuming the same dominant mechanism as before, Ishii and Grolmes (1975) developed a criterion for droplet entrainment based on a Reynolds number depending on the geometry. However, in all the cases, the shearing off of roll wave crests was the only mechanism and regime to be studied. As shown in Table III, one of the most important results is the minimum Reynolds number, below which no entrainment occurs. This is a function of $y^+$ ($y^+$ represents the dimensionless distance from the wall based on the shear velocity, which cannot be established with precision; it might vary in the range 15 to 7.5). Okawa et al. (2002) obtained an entrainment function that was corroborated with 17 different experiments under different operational conditions. However, in the equation presented in Table III, the values of $k_E$ and $k_D$ are unknown. In order to calculate them, several correlations have to be used, which in some cases could have about 30% error. Nevertheless, the results obtained with this correlation are in good agreement with the experimental information available with an error of $\pm 15\%$.

The major drawbacks of all the entrainment kernels are related to the hypotheses or assumptions invoked when developing the mathematical expressions. One hypothesis that is very relevant is related to the type of eddy, or flow regime, that will produce entrainment. Also, in several cases, the geometry of the system had to be taken into consideration when the entrainment expressions were obtained. This makes the correlation apparatus dependent and almost impossible to extrapolate to other geometries. Kataoka et al. (2000), for example, have proposed a correlation

Downloaded by [Norges Landbrukshoegskole], [Dr Jorge Marchetti] at 03:35 20 April 2012

**Table III.** Entrainment correlations

| Mathematical expression | Assumptions-limitations | Reference |
|---|---|---|
| $\dot{\varepsilon} = 3.54 \times 10^{-3} \left( \frac{\varsigma_i}{\sigma} \left( \frac{j_f}{\sigma} \right)^{0,6} \right)^{0,57}$ for $\frac{\varsigma_i}{\sigma} \left( \frac{j_f}{\sigma} \right)^{0,6} > 120$ | The term $(j_f/\sigma)$ is not based on a physical mechanism; restricted application to other cases | Ueda (1979) |
| $\frac{D_p}{j_g} = 0.022 \mathrm{Re}_g^{-0.25} \left( \frac{M}{\rho_f} \right)^{-0.26} \left( \frac{\rho_g}{\rho_f} \right)^{0.26}$ | Based on physical information of the system | Paleev and Filippovich (1966) |
| $\dot{\varepsilon} = 0.935 \times 10^{-5} \zeta \exp(-1.87 \times 10^{-5} \zeta) \rho_f j_f \times \mathrm{Re}_f^{0.5} We^{-0.25} E_\infty + 0.022 \rho_f j_f \mathrm{Re}_f^{-0.26} \times \left( \frac{\mu_g}{\mu_f} \right)^{0.26} E_\infty^{0.74} (1 - \exp(-1.87 \times 10^{-5} \zeta^2))^{0.74}$ | Expression based on axial location and operational conditions and not in local flow conditions | Katoaka et al. (2000) |
| $\frac{\dot{\varepsilon} D_h}{\mu_f} = 6.6 \times 10^{-7} \mathrm{Re}_f^{0.74} We^{0.925} \mathrm{Re}_{ff}^{0.185} \left( \frac{\mu_g}{\mu_f} \right)^{0.26}$ for $z > 440 D_h We^{0.25} / \mathrm{Re}_f^{0.5}$ | For regions away from the entrance | Katoaka et al. (2000) |
| $\mathrm{Re}_c = \exp \left[ 5.85 + 0.425 \frac{\mu_g}{\mu_f} \left( \frac{\rho_f^0}{\rho_g^0} \right)^{0.5} \right]$ | Does not consider gravity forces | Hewitt and Govan (1990) |
| $\dot{\varepsilon} \sim \left( \frac{j_f D_h \rho_f}{\mu_f} \right)^{0.25} \left( \left( \frac{j_g^2 D_h \rho_g}{\sigma} \right) \left( \frac{\rho_f - \rho_g}{\rho_g} \right)^{1/2} \right)^{1.25}$ | There is no critical liquid or gas flow; includes influence of liquid viscosity | Ishii and Mishima (1989) |
| $\mathrm{Re}_{f_{\min}} = \left( \frac{y^+}{0.347} \right)^{3/2} \left( \frac{\rho_f}{\rho_g} \right)^{3/4} \left( \frac{\mu_g}{\mu_f} \right)^{3/2}$ | Below this Reynolds number there is no entrainment; $y^+$ cannot be established | Ishii and Grolmes (1975) |
| $\frac{E_\infty}{1 - E_\infty} = \frac{1}{4} \frac{k_E}{k_D} \frac{\sqrt{f_i f_w} \sqrt{\rho_l \rho_g} J_g^2 D_t}{\sigma} \left( \frac{\rho_l}{\rho_g} \right)^n$ | Captures the overall trends of the system | Okawa et al. (2002) |
| $m_e = 1.07 \left( \frac{\varsigma_{fg} \Delta h_{eq}}{\sigma} \right) \left( \frac{\mu_g \mu_f}{\sigma} \right) \left( \frac{\rho_f}{\rho_g} \right)^{-0.5}$ | Low-pressure steam-water two-phase systems | Sugawara (1990) |

that is suitable for annular flow and for a water-nitrogen system. Nevertheless, it might be possible, as shown by Patruno et al. (2010), that by rewriting the dimensionless correlations, more general expressions for several geometries and different mixtures could be obtained.

As in the case for breakage kernels (Table II), in Table III, for the entrainment rate expression, it could be also seen that each case has several assumptions and restrictions that are not the same for all cases, mainly since there are geometrical differences and also different liquids and gases used for the experiments. The differences mean that each case is not correlated with the others, making it almost impossible to compare them.

Downloaded by [Norges Landbrukshoegskole], [Dr Jorge Marchetti] at 03:35 20 April 2012

## Droplet Deposition

Droplet deposition and re-entrainment are phenomena that occur in many places in process plants. At steady state, the relative rates of these two processes determine liquid holdup and influence pressure drops. In order to better understand the phenomena of deposition, Figure 9 shows a diagram of the physical situation where a droplet interacts with a wall. The effect of the wall, if it is wet or not, has no significant effect on this schematic representation; however, it does have an effect on the operation conditions and when deposition might occur instead of bouncing. Figure 10, on the other hand, shows a particle deposition scenario. In this case, a smaller droplet will bounce back, while some of the initial mass is attached to the wall or the film.

Correlations for deposition rates and efficiencies can be found in the literature, and a selection of these is summarized below. Mundo et al. (1995) proposed the following criterion (Equation (20)) equation based on the Ohnesorge and Reynolds numbers. This model is based on the impact momentum of the droplets hitting a dry wall. However, since this model is energy dependent, it is important to note that the type and properties of the surface are important and may modify the value of $K_c$ (critical value according to Equation (21)) as determined by Cossali et al. (1997).

$$K_C = Oh \times \mathrm{Re}^{1.25} \tag{20}$$

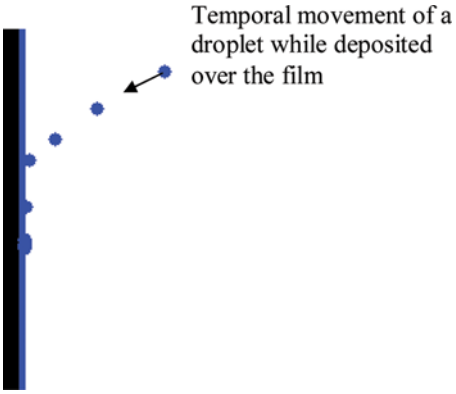


**Figure 9.** Deposition of a liquid droplet. (Figure provided in color online.)

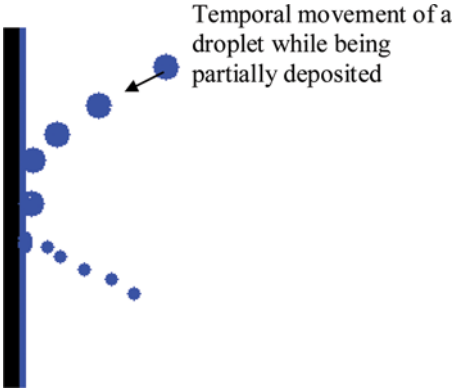


**Figure 10.** Partial deposition of a liquid droplet. (Figure provided in color online.)

If the possibility of deposition on liquid films is taken into account, then the deposition efficiency needs to be modified, depending on the liquid film thickness, as done by Coghe et al. (1995), and the correlation changes into the following criterion:

$$WeLa^{0.2} \geq 1900 + 6240\delta_f^{1.4} \tag{21}$$

It is important to note that this equation considers that secondary droplets could also interact with the film if the term $WeLa^{0.2}$ is larger than the right-hand side.

O'Rourke and Amsden (2000) studied this effect and concluded that a parameter called the splash number (E) is needed. They corroborate what was previously established by Yarin and Weiss (1995):

$$\tilde{E}^2 = We_{imp} \frac{1}{\min\left(\delta_f / d_{prim}, 1\right) + \delta_{bl}/d_{prim}} > 3329.29 \tag{22}$$

Morud (2005) obtained an expression for the deposition rate of droplets as a function of the shear stress ($u^*$) and a dimensionless relaxation time. The deposition rate is given as:

$$R_D = V_w C_d \tag{23}$$

where $C_d$ is the droplet volume concentration and $V_w = \Pi/\sqrt{2\pi}$ and $\sigma$ is defined as follows:

$$\begin{aligned}
\frac{\Pi}{u^*} &= \sqrt{2\pi} \times 1.3 \times 10^{-5} \qquad \text{for } \tau^+ < 0.2 \\
\frac{\Pi}{u^*} &= \sqrt{2\pi} \times 3.25 \times 10^{-4} (\tau^+)^2 \text{ for } 0.2 < \tau^+ < 22.9 \\
\frac{\Pi}{u^*} &= \sqrt{2\pi} \times 0.17 \qquad \text{for } 22.9 < \tau^+ < 14751 \\
\frac{\Pi}{u^*} &= \sqrt{2\pi} \times 20.7/\sqrt{\tau^+} \qquad \text{for } \tau^+ > 14751
\end{aligned} \tag{24}$$

where

$$\tau^+ = \frac{1}{18} \frac{\rho_{drop}}{\rho_g} \left( \frac{d_{drop} \rho_g u^*}{\mu_g} \right)^2$$

Downloaded by [Norges Landbrukshoegskole], [Dr Jorge Marchetti] at 03:35 20 April 2012

Downloaded by [Norges Landbrukshoegskole], [Dr Jorge Marchetti] at 03:35 20 April 2012

For this model, the velocities of the droplets, individually considered, perpendicular to the wall are assumed to follow a normal distribution, while the standard deviation ($\sigma$) is determined for each particular case.

McCoy and Hanratty (1977) developed a relationship between the deposition rate $k_d$ and dimensionless numbers for dilute particle concentrations when entrance and electrical effects as well as wall roughness effects are disregarded. They also showed that the value of $k_d$ varies inversely with the particle diameter for very large particles. However, to develop this equation, constant droplet size as well constant deposition velocity were assumed constant. The relation for vertical axial flow is given as:

$$\frac{R_d}{\Xi^*} = 20.7\left(R_t^+\right)^{-0.5}$$
where
$$R_t^+ = \frac{d_p^2 \rho_g \rho_p (U^*)^2}{18\mu_g^2} \tag{25}$$

Kneem and Strauss (1969) performed experimental work on the deposition of fine particles onto a solid surface. The obtained experimental data were correlated with a simple expression based on the absence of gravitational or external forces, valid for particles between 0.5 and 50 μm. The expression is as follows:

$$\frac{N_o}{\mu_\tau \bar{c}} \propto S_*^2 \tag{26}$$

where No is the particle flow to the surface, $\mu_\tau$ is the shear velocity, $c$ is the mean concentration, and $S_*$ is the dimensionless stopping distance, defined as:

$$S_* = 0.05\left(\frac{\mu_\tau d}{\upsilon}\right)^2 \frac{\sigma}{\rho} \tag{27}$$

Here d is the particle diameter, $\upsilon$ is the fluid viscosity, and $\sigma/\rho$ is the relative density of particle to fluid. This expression showed good agreement with the experimental data. Despite good agreement between model and experimental data, the authors arrived at three main conclusions in the development of predictive kernels for deposition: (1) the properties of the fluids close to the wall are of extreme relevance for determining the deposition rate, (2) particles have inertia and this needs to be considered, and (3) the size of the particles is needed in order to determinate if Brownian motion is important.

Several other kernels can be found in the literature, such as those provided by Liu and Agarwal (1974), Okawa and Kataoka (2005), and Friedlander and Johnstone (1957).

Regarding the models discussed in this article for deposition of droplets on a wall or a liquid film, the main drawback is that there is no general expression allowing starting with a dry surface that will at some point start to get wet due to previous splashing. Moreover, Equation (26) does not show that some droplets might bounce back and some might partially coalesce (part of the droplet is included in the film, part of the droplet bounces back to the main flow).

Downloaded by [Norges Landbrukshoegskole], [Dr Jorge Marchetti] at 03:35 20 April 2012

## Conclusions

The phenomena of entrainment is quite complex to model; therefore, several kernels were found in the literature, and there is not a unique mathematical representation that will allow predicting the behavior for all cases. Most kernels are associated with physical properties of the system, making them case dependent.

Deposition kernels are not as abundantly studied in the literature as entrainment kernels. Several physical properties of the system are crucial to determine if deposition will occur or not, making this phenomenon property dependent. The characteristics of the wall roughness, physics properties, if the wall is wet or dry, just to name some, influence the rate of deposition of droplets.

Due to velocity changes, the interaction of one droplet with another one could have different outcomes. As shown, one of the options is coalescence of droplets. If this phenomenon takes place at the end of a separation plant, when only very small droplets remain, there is a significant chance that bigger and undesired droplets will be produced, generating a complication for the process.

However, if head-on and head-off collisions occur, there will be smaller droplets generated, produced from the lost of mass of the initial father droplets.

From all the previous work, it can be seen that several kernels have been found to correlate experimental information. However, because the behavior is dependent on the physical-chemical properties of the system and fluids, kernels are physically dependent on the system used, and, therefore, the results are restricted to those scenarios only.

Inverse problem solutions are also used; nevertheless, they are more problem dependent because the mathematical solution is based on experimental information. Correlation between physical properties of different systems and how kernels are modified with them as well as the possibility of finding new independents kernels on the system are the next challenge.

As pointed out in Table II for breakage and Table III for entrainment, several authors have used different experimental setups as well as different fluids. This difference makes the comparison among the different kernels almost impossible due to the experimental-setup dependency of the mathematical expression developed. One general kernel, based on the physics and not the problem, has not yet been found.

## Acknowledgments

The postdoctoral fellowship of J. M. Marchetti, financed by the Research Council of Norway, Petromaks programme, through the project HiPGLS (169477), is gratefully appreciated.

## Nomenclature

| | |
|---|---|
| A | mathematical constant |
| Amp | amplitude |
| B | mathematical constant |
| b | mathematical constant |
| Cd | droplet concentration |
| $c_i$ | mathematical constant |
| $C_i$ | mathematical constant |
| d | droplet diameter |

Downloaded by [Norges Landbrukshoegskole], [Dr Jorge Marchetti] at 03:35 20 April 2012

| | |
|---|---|
| D | stirred diameter |
| $d_0$ | father's diameter |
| $d_1$ | diameter of first droplet that interacts |
| $d_2$ | diameter of second droplet that interacts |
| $d_c$ | critical diameter that produced a maximum in the breakage |
| $D_h$ | hydraulic diameter |
| Di | impeller diameter |
| $D_p$ | deposition factor |
| $d_p$ | particle diameter |
| Dt | tube diameter |
| E | splash number |
| $E_\infty$ | equilibrium value of fractional entrainment |
| Ec | activation energy |
| $f_{bv}$ | volume of the second daughter |
| $f_i$ | friction factor of interface |
| $f_w$ | friction factor of wall |
| H | height of reservoir |
| h | real area that is in contact during the collision |
| I | mathematical constant |
| $I_p$ | impact factor |
| $j_f$ | volumetric flux of the film |
| $j_g$ | volumetric flux of the gas |
| Jg | dimensionless gas flux |
| k | wave number |
| $k_i$ | mathematical constants |
| L | distance between droplets' centers |
| l | characteristic length, normally, droplet diameter |
| La | Laplace number |
| M | mass of liquid content in 1 kg of gas |
| $Mk_d$ | mass transfer coefficient of gas |
| $Mk_e$ | mass transfer coefficient of entrained droplet |
| N | rotational frequency of impeller |
| Oh | Ohnesorge number |
| $R_d$ | deposition rate |
| $Re_{ff}$ | Reynolds number of total liquid |
| $Re_f$ | Reynolds number of liquid |
| $Re_g$ | Reynolds number of gas phase |
| Rt | relaxation time |
| T | diameter of reservoir |
| u | relative velocity across the mean diameter d |
| $u^*$ | shear stress |
| v | velocity |
| We | Weber number |
| x | dimensionless impact factor |
| z | axial distance from the entrance |

***Greek Letters***

| | |
|---|---|
| $\beta$ | mathematical constant |
| $\delta_f$ | film thickness |

| | |
|---|---|
| $\dot{\varepsilon}$ | entrainment rate |
| $\varepsilon$ | local average dissipation per unit mass |
| $\zeta$ | dimensionless distance |
| $\Delta h_{eq}$ | wave height |
| $\theta$ | angle between relative velocity and center-to-center line |
| $\kappa$ | eccentricity |
| $\mu_c$ | viscosity of continuous phase |
| $\mu_d$ | viscosity of dispersed phase |
| $\mu_f$ | viscosity of film |
| $\mu_g$ | viscosity of gas phase |
| $\xi$ | ratio between eddy and droplet diameter |
| $\Xi^*$ | friction velocity |
| $\rho$ | density |
| $\rho_d$ | density of discrete phase |
| $\rho_{drop}$ | density of droplet |
| $\rho_f$ | density of film |
| $\rho_g$ | density of gas phase |
| $\rho_p$ | density of particle |
| $\sigma$ | surface tension |
| $\varsigma_i$ | interfacial shear stress |
| $\tau$ | standard deviation |
| $\upsilon$ | volume of daughter droplet |
| $\varphi$ | dispersed phase holdup fraction |
| $\Psi$ | angle between both centers |
| $\omega$ | deviation parameter |
| $\Omega$ | axial diameter ratio |

## References

Alipchenkov, V. M., Nigmatulin, R. I., Soloviev, S. L., Stonik, O. G., Zaichik, L. I., and Zeigarnik, Y. A. (2004). A three-fluid model of two-phase dispersed-annular flow, *Int. J. Heat Mass Transfer*, **47**, 5323–5338.

Ashgriz, N., and Poo, J. Y. (1990). Coalescence and separation in binary collision of liquid drops, *J. Fluids Mech.*, **221**, 183–204.

Austrheim, T., Gjertsen, L. H., and Hoffman, A. C. (2007). Re-entrainment correlations for demisting cylcones acting at elevated pressures on a range of fluids, *Energy Fuel*, **21**, 2969–2976.

Austrheim, T., Gjertsen, L. H., and Hoffman, A. C. (2008a). Experimental investigation of the performance of a large-scale scrubber operating at elevated pressure on live natural gas, *Fuel*, **87**(7), 1281–1288.

Austrheim, T., Gjertsen, L. H., and Hoffman, A. C. (2008b). An experimental investigation of scrubber internals at conditions of low pressure, *Chem. Eng. Sci.*, **138**, 95–102.

Kolev, N. I. (2002). *Multiphase Flow Dynamics 2: Mechanical and Thermal Interactions*, Springer, Berlin.

BP. (2006). *BP Statistical Review of World Energy 2006*, BP, London.

Brazier-Smith, P. R., Jennings, S. G., and Latham, J. (1972). The interaction of falling water drops: Coalescence, *Proc. R. Soc. Lond. A*, **326**, 393–408.

Bürkholz, A. (1989). *Droplet Separation*, VCH Publications, New York.

Chesters, A. K. (1991). Modelling of coalescence processes in fluid-liquid dispersions. A review of current understanding, *Chem. Eng. Res. Des.*, **69**(4), 259–227.

Downloaded by [Norges Landbrukshoegskole], [Dr Jorge Marchetti] at 03:35 20 April 2012

Coghe, A., Cossali, G. E., and Marengo, M. (1995). A first study about single drop impingement on thick liquid film in a low Laplace number range, in *Proceedings of PARTEC'95, Nürnberg*.

Cossali, G. E., Coghe, A., and Marengo, M. (1997). The impact of a single drop on a wetted surface, *Exp. Fluids*, **22**, 463–472.

Coulaloglou, C. A., and Tavlarides, L. L. (1977). Description of interaction processes in agitated liquid-liquid dispersions, *Chem. Eng. Sci.*, **32**, 1289–1297.

Dorao, C. A., Patruno, L. E., Dupuy, P. M., Jakobsen, H. A., and Svendsen, H. F. (2008). Modelling of droplet-droplet interaction phenomena in gas-liquid systems for natural gas processing, *Chem. Eng. Sci.*, **63**, 3585–3592.

Estrade, J. P., Carentz, H., Lavergne, G., and Biscos, Y. (1999). Experimental investigation of dynamic binary collision of ethanol droplets—A model for droplet coalescence and bouncing, *Int. J. Heat Fluid Flow*, **20**, 486–491.

Friedlander, S. K., and Johnstone, H. F. (1957). Deposition of suspended particles from turbulent gas streams, *Ind. Eng. Chem.*, **49**, 1151–1156.

Gelfand, B. E. (1996). Droplet breakup phenomena in flows with velocity lag, *Prog. Energy Combust. Sci.*, **22**, 201–265.

Georjon, T. L., and Reitz, R. D. (1999). A drop-shattering collision model for multidimensional spray computations, *At. Sprays*, **9**, 231–245.

Gotaas, C., Havelka, P., Jakobsen, H. A., and Svendsen, H. F. (2007a). Evaluation of impact parameter in droplet-droplet collision experiments by the aliasing method, *Phys. Fluids*, **19**(10), 102105.

Gotaas, C., Havelka, P., Jakobsen, H. A., and Svendsen, H. F. (2007b). Effect of viscosity on droplet-droplet collision outcome: Experimental study and numerical comparison, *Phys. Fluids*, **19**, 102106.

Hesketh, R. P., Etchells, A. W., and Russell, T. W. F. (1991). Bubble breakage in pipeline flow, *Chem. Eng. Sci.*, **46**, 1–9.

Hewitt, G. F., and Govan, A. H. (1990). Phenomenological modelling of non-equilibrium flows with phase change, *Int. J. Heat Mass Transfer*, **33**, 229–242.

Hsia, A. M., and Tavlarides, L. L. (1983). Simulation analysis of drop breakage, coalescence and micromixing in liquid-liquid stirred tanks, *Chem. Eng. J.*, **26**, 189–199.

Jakobsen, H. A. (2008). *Chemical Reactor Modeling: Multiphase Reactive Flows*, Springer, Berlin.

Ishii, M., and Grolmes, M. A. (1975). Inception criteria for droplet entrainment in two-phase concurrent film flow, *AIChE J.*, **21**(2), 308–318.

Ishii, M., and Mishima, K. (1989). Droplet entrainment correlation in annular two-phase flow, *Int. J. Heat Mass Transfer*, **32**, 1835–1846.

Johnsen, C. G. (2007). Experimental and numerical investigation of droplet phenmomena, PhD diss., Faculty of Natural Science and Technology of Norway, Trondheim, Norway.

Kataoka, I., Ishii, M., and Nakayama, A. (2000). Entrainment and deposition rates of droplets in annular two-phase flow, *Int. J. Heat Mass Transfer*, **43**, 1573–1589.

Kidnay, A. J., and Parrish, W. R. (2006). *Fundamentals of Natural Gas Processing*, Taylor & Francis, Boca Raton, Fla.

Kneen, T., and Strauss, W. (1969). Deposition of dust from turbulent gas streams, *Atmos. Environ.*, **3**, 55–67.

Kollár, L. E., Farzaneh, M., and Karev, A. R. (2005). Modelling droplet collision and coalescence in an icing wind tunnel and the influence of these processes on droplet size distribution, *Int. J. Multiph. Flow*, **31**, 69–92.

Konno, M., Matsunaga, Y., Arai, K., and Saito, S. (1980). Simulations model for break-up process in an agitated tank, *J. Chem. Eng. Jpn.*, **13**, 67–73.

Konno, M., Aoki, M., and Saito, S. (1983). Scale effect on break-up process in liquid-liquid agitated tanks, *J. Chem. Eng. Jpn.*, **13**, 312–319.

Downloaded by [Norges Landbrukshoegskole], [Dr Jorge Marchetti] at 03:35 20 April 2012

Lasheras, J. C., Eastwood, C., Martínez-Basán, C., and Montañés, J. L. (2002). A review of statistical models for the break-up of an immiscible fluid immersed into a fully developed turbulent flow, *Int. J. Multiph. Flow*, **28**, 247–278.

Lee, C. H., Erickson, L. E., and Glasgow, L. A. (1987). Dynamics of bubble size distribution in turbulent gas-liquid dispersions, *Chem. Eng. Commun.*, **61**, 181–195.

Liu, B. Y. H., and Agarwal, J. K. (1974). Experimental observations of aerosol deposition in turbulent flow, *J. Aerosol Sci.*, **5**, 145–155.

Lopez de Bertodano, M. A., Jan, C. S., and Beus, S. G. (1997). Annular flow entrainment rate experiment in a small vertical pipe, *Nucl. Eng. Des.*, **178**, 61–70.

Luo, H., and Svendsen, H. F. (1996). Theoretical model for drop and bubble break-up in turbulent dispersions, *AIChE J.*, **42**, 1225–1233.

Martinéz-Basán, C., Montanes, J. L., and Lasheras, J. C. (1999). On the breakup of an air bubble injected into a fully developed turbulent flow: Part 1: Break-up frequency, *J. Fluid Mech.*, **401**, 157–182.

McCoy, D. D., and Hanratty, T. J. (1977). Rate of deposition of droplets in annular two-phase flow, *Int. J. Multiph. Flow*, **3**, 319–331.

Morud, J. (2005). Dilute gas-liquid flows with liquid films on walls, paper presented at Fourth International Conference on CFD in the Oil and Gas, Metallurgical & Process Industries, SINTEF/NTNU, Trondheim, Norway.

Mundo, C., Sommerfeld, M., and Tropea, C. (1995). Droplet-wall collisions: Experimental studies of the deformation and breakup process, *Int. J. Multiph. Flow*, **21**, 151–173.

Nambiar, D. K. R., Kumar, R., Das, T. R., and Gandhi, K. S. (1992). A new model for the breakage frequency of drops in turbulent stirred dispersions, *Chem. Eng. Sci.*, **47**, 2989–3002.

Nigmatulin, R. I., Nigmatulin, B. I., Khodzhaev, Ya. D., and Kroshilin, V. E. (1996). Entrainment and deposition rate in a dispersed-film flow, *Int. J. Multiph. Flow*, **22**(1), 19–30.

Okawa, T., and Kataoka, I. (2005). Correlations for the mass transfer rate of droplets in vertical upward annular flow, *Int. J. Heat Mass Transfer*, **48**, 4766–4778.

Okawa, T., Kitahara, T., Yoshida, K., Matsumoto, T., and Kataoka, I. (2002). New entrainment rate correlation in annular two-phase flow applicable to wide range of flow condition, *Int. J. Heat Mass Transfer*, **45**, 87–98.

Orme, M. (1997). Experiments on droplet collisions, bounce, coalescence and disruption, *Prog. Energy Combust. Sci.*, **23**, 65–79.

O'Rourke, P. J. (1981). Collective drop effects in vaporizing liquid spray, PhD diss., Dept. Mechanical and Aerospace Engineering, Princeton University.

O'Rourke, P. J., and Amsden, A. A. (2000). A spray/wall interaction submodel for the KIVA-3 wall film mode, SAE paper no. 2000-01-0271, SAE, Warrendale, Penn.

Paleev, J. J., and Filippovich, B. S. (1966). Phenomena of liquid transfer in two-phase dispersed annular flow, *Int. J. Heat Mass Transfer*, **9**, 1089–1093.

Pan, L., and Hanratty, T. J. (2002). Correlation of entrainment for annular flow in vertical pipes, *Int. J. Multiph. Flow*, **28**, 363–384.

Pan, Y., and Suga, K. (2005). Numerical simulation of binary liquid droplet collision, *Phys. Fluids*, **17**, 082105.

Park, H., Yoon, S. S., Jepsen, R. A., Heister, S. D., and Kim, H. Y. (2008). Droplet bounce simulations and air pressure effects on the deformation of pre-impact droplets, using a boundary element method, *Eng. Anal. Bound. Elem.*, **32**, 21–31.

Patruno, L. E., Dorao, C. A., Dupuy, P. M., Svendsen, H. F., and Jakobsen, H. A. (2009a). Identification of droplet breakage kernel for population balance modelling, *Chem. Eng. Sci.*, **64**(4), 638–645.

Patruno, L. E., Dorao, C. A., Svendsen, H. F., and Jakobsen, H. A. (2009b). Analysis of breakage kernels for population balance modelling, *Chem. Eng. Sci.*, **64**(3), 501–508.

Patruno, L. E., Marchioro Ystad, P. A., Marchetti, J. M., Dorao, C. A., Svendsen, H. F., and Jakobsen, H. A. (2010). Liquid entrainment-droplet size distribution for a low surface tension mixture. (Unpublished data).

Downloaded by [Norges Landbrukshoegskole], [Dr Jorge Marchetti] at 03:35 20 April 2012

Post, S. L., and Abraham, J. (2002). Modelling the outcome of drop-drop collision in diesel spray, *Int. J. Multiph. Flow*, **28**, 997–1019.

Prince, M. J., and Blanch, H. W. (1990). Bubble coalescence and break-up in air-sparged bubble columns, *AIChE J.*, **36**, 1485–1499.

Qian, J., and Law, C. K. (1997). Regimes of coalescence and separation in droplet collision, *J. Fluid Mech.*, **331**, 59–80.

Ramkrishna, D. (2000). *Population Balances: Theory and Applications to Particle Systems in Engineering*, Academic Press, San Diego, Calif.

Renardy, Y., Popinet, S., Duchemin, L., Renardy, M., Zaleski, S., Josserand, C., Drumright-Clarke, M. A., Richard, D., Clanet, C., and Quéré, D. (2003). Pyramidal and toroidal water drops after impact on a solid surface, *J. Fluid Mech.*, **484**, 69–83.

Sathyagal, A. N., Ramkrishna, D., and Narsimhan, G. (1996). Droplet breakage in stirred dispersions. Breakage functions from experimental drop-size distributions, *Chem. Eng. Sci.*, **51**(9), 1377–1391.

Sawant, P., Ishii, M., and Mori, M. (2008). Droplet entrainment correlation in vertical upward co-current annular two-phase flow, *Nucl. Eng. Des.*, **238**, 1342–1352.

Sovova, H. (1981). Breakage and coalescence of drops in a batch stirred vessel: II. Comparison of model and experiments, *Chem. Eng. Sci.*, **36**(9), 1567–1573.

Sugawara, S. (1990). Droplet deposition and entrainment modelling based on the three-fluid model, *Nucl. Eng. Des.*, **122**, 47–84.

Tennison, P. J., Georjon, T. L., Farrell, P. V., and Reitz, R. D. (1998). An experimental and numerical study of sprays from a common rail injection system for use in an HSDI diesel engine, SAE Technical Paper 980810, SAE, Warrendale, Penn.

Tsouris, C., and Tavlarides, L. L. (1994). Breakage and coalescence models for drops in turbulent dispersions, *AIChE J.*, **40**(3), 395–406.

Ueda, T. (1979). Droplet entrainment rate and droplet diameter in annular two-phase flow, *Jpn. Soc. Mech. Eng.* **45**(389), 127–135.

Valentas, K. J., Bilous, O., and Amundson, N. R. (1966). Analysis of breakage in dispersed phase systems, *Ind. Eng. Chem. Fundam.*, **5**, 271–279.

Xie, H., Koshizuka, S., and Oka, Y. (2004). Numerical simulation of liquid drop deposition in annular-mist flow regime of boiling water reactor, *J. Nucl. Sci. Technol.*, **41**(5), 569–578.

Yarin, A. L., and Weiss, D. A. (1995). Impact of drops on solid surface: Self-similar capillary waves and splashing as a new type of kinematic discontinuity, *J. Fluid Mech.*, **283**, 141–173.

Downloaded by [Norges Landbrukshoegskole], [Dr Jorge Marchetti] at 03:35 20 April 2012